International Journal of Concrete Structures and Materials
Vol.9, No.1, pp.69–88, March 2015
DOI 10.1007/s40069-014-0088-x
ISSN 1976-0485 / eISSN 2234-1315

Performance of High Strength Self-Compacting Concrete Beams under Different Modes of Failure

Raya Hassan Harkouss*, and Bilal Salim Hamad

(Received March 7, 2014, Accepted August 18, 2014, Published online October 1, 2014)

Abstract: Self-consolidating concrete (SCC) is a stable and cohesive high consistency concrete mix with enhanced filling ability properties that reduce the need for mechanical compaction. Limited standards and specifications have been reported in the literature on the structural behavior of reinforced self-compacting concrete elements. The significance of the research presented in this paper stems from the need to investigate the effect of enhanced fluidity of SCC on the structural behavior of high strength self-consolidating reinforced concrete beams. To meet the objectives of this research, twelve reinforced concrete beams were prepared with two different generations of superplasticizers and designed to exhibit flexure, shear, or bond splitting failure. The compared beams were identical except for the type of superplasticizer being used (second generation sulphonated-based superplasticizer or third generation polycarboxylate-based superplasticizer). The outcomes of the experimental work revealed comparable resistance of beam specimens made with self-compacting (SCC) and conventional vibrated concrete (VC). The dissimilarities in the experimental values between the SCC and the control VC beams were not major, leading to the conclusion that the high flowability of SCC has little effect on the flexural, shear and bond strengths of concrete members.

Keywords: construction materials, concrete admixtures, self-consolidating concrete, high-strength concrete, reinforced concrete beams, structural behavior.

1. Introduction

Self-consolidating concrete (SCC) is distinguished by its high fluidity, passing ability and cohesiveness characteristics that eliminate or reduce to a minimum the need for mechanical compaction. Reducing the intervention of the human factor in the concreting stage improves the quality of the project under construction.

The advantages associated with SCC have led to the adoption of this relatively advanced technology in many contemporary projects, even before the release of specifications, testing techniques and standards that reflect the behavior of structural elements cast using high consistency concrete.

The research reported in this paper is concerned with the effect of enhanced fluidity of SCC on the structural behavior of reinforced concrete beam elements designed to exhibit different critical modes of failure. The hypothesis to be tested is whether the high consistency of SCC will negatively affect the shear strength of reinforced SCC members and the bond strength of spliced bars in such members.

Department of Civil and Environmental Engineering, American University of Beirut, Riad El-Solh, Beirut 1107-2020, Lebanon.
*Corresponding Author; E-mail: rhharkouss@darbeirut.com

Accordingly, a three-phase research program was conducted to study the effect of two types of superplasticizers on the mechanical performance of plain and reinforced concrete elements. Sulphonated naphtalene formaldehyde-based (SNF) admixture was chosen to represent the conventional type of second generation superplasticizer commonly used by the concrete industry in the production of high strength workable concrete. On the other hand, polycarboxylate ethers-based superplasticizer (PCE), a high range water reducing admixture, was the third generation superplasticizer incorporated in the development of the SCC mixes in this research.

The difference in the dispersion mechanisms of the second and third generation superplasticizers is expected to reflect on the mechanical properties of concrete, a point that was elaborated in Phases 1 and 2 of the AUB research program. To limit the number of variables merely to the type of admixture used in the concrete mix, the experiments of the first two phases of the research aimed at establishing an optimum mix design with a common dosage of second or third generation superplasticizer that would ensure the minimum workability characteristics for vibrated concrete (VC) and the high consistency properties for SCC. In the first phase, comparative studies of high strength mortar mixes prepared with second generation (SNF) or third generation (PCE) superplasticizer were conducted. In the second phase, the comparative studies were carried on concrete mixes rather than mortar mixes. The two studies unveiled that a dosage of 1.6 % of second generation or third generation superplasticizer is satisfactory.

The research reported in this paper constitutes the third phase of the experimental program. It investigates and compares the structural behavior of reinforced concrete beams cast using the optimal high strength SCC and VC mixes established in the first two phases of the research with a second generation (SNF) or third generation (PCE) superplasticizer content of 1.6 % of the total weight of cement.

2. Literature Review

Few studies were found dealing with high strength SCC beams produced using PCE based admixtures. A common procedure was followed in the majority of these studies where beams prepared with SCC, frequently comprising fly ash or silica fume powders, were compared with control beams cast using VC mixes made with different constituents and mix proportions. The overlapping effect of the numerous variables engaged in those studies often resulted in losing the track on the effect of each variable on the behavior of the reinforced concrete specimens.

The majority of the research reported in the literature review agreed on the equivalence of the bond strength between normal concrete and SCC (Domone 2006). Desnerck et al. (2010). studied the bond characteristics of different bar diameters in beam specimens cast using self-compacting concrete SCC and conventional vibrated concrete VC having an $f_c^{'}$ of approximately 60 MPa. The concrete mixes were designed differently where SCC mixes involved PCE superplasticizers and limestone fillers, two additional constituents that were excluded from the conventional VC mix design. The aggregate distribution of VC and SCC mixes was also different. The outcomes of the research study concluded on the similarity of the bond strength between VC and SCC beams for large bar diameters whereas the bond strengths for SCC appeared to be superior in beams with small bar diameters.

Turk et al. (2008) also inspected the bond strength of tension lap splices in SCC beams. Beam specimens with 16 and 20 mm bars were used to compare the behavior of SCC and VC elements having a compressive strengths ranging from 41.5 to 44 MPa. The stability of SCC mixes was maintained using silica fume. The self-compactness of concrete was attained using PCE superplasticizer whereas sulphonated melamine-based superplasticizer was used for the normal concrete mix. Different concrete mix proportions were adopted. The study led to a conclusion that the enhanced filling ability of SCC results in higher bond strengths.

Foroughi-Asl et al. (2008) reported on pullout tests designed to study the effect of SCC on bond strengths. Different bar diameters were tested. The mix designs of the SCC and the companion normal concrete NC specimens were the same except for the addition of the silica fume and PCE superplasticizers in the SCC specimens. The experimental data gathered revealed slightly higher bond strengths for the SCC specimens.

This similarity in the behavior of SCC and normal concrete specimens was not reflected in the research papers studying the shear resistance of reinforced concrete beam elements. The shear capacity of normal VC appeared to overcome that of SCC. Veerle Boel (2010) tested the shear capacity of beam specimen made with SCC and VC. The SCC mix proportions were marked by the high limestone filler content and the low river gravel volumes. The SCC specimen contained 43 % lower aggregate content. Boel associated the lower shear capacity of the SCC beams to the lower aggregate interlock caused by the fewer coarse aggregates.

Hassan et al. (2008) also conducted an experimental investigation on the shear strength of SCC beams. The concrete mixes were designed differently where SCC contained 25 % coarse aggregate content lower than NC. The difference in volume dedicated for coarse aggregate was compensated by an addition in the sand content of the SCC mixes. The experimental results indicated a similarity in the overall failure mode in terms of the cracking pattern, crack width and height in SCC and NC beams. The ultimate shear capacity of SCC beams appeared to be lower than their NC counterparts. According to the researchers, the lower shear strength could be attributed to the decrease in coarse aggregate content that used to provide additional resistance to shear through aggregate interlock mechanisms.

Sharifi (2012) studied the flexural behavior of SCC beams having an average concrete compressive strength of 30 MPa. SCC mixes included micro silica and limestone powder to control the mix stability. According to the researcher, the theoretical calculations regularly followed to find the moment capacity of reinforced concrete beams are conservative and reliable in the estimation of SCC beam capacities.

The involvement of different types of fillers in the concrete mix design, as mentioned in the previous reported research, has an impact on the hydration of cement and consequently on the concrete microstructure and the hardened concrete properties. In addition, the use of different mix proportions and the variation in the type of coarse aggregates (river gravel or crushed limestone) will also affect the properties of concrete and its behavior in handling the tensile stresses at the microstructural level. Accordingly, conclusions related to the effect of enhanced consistency of SCC mixes drawn from the comparison studies between SCC and conventional vibrated concrete would be more reliable if identical mix constituents are used to avoid any factors that might affect the structural behavior.

3. Research Objectives

The main objective of the research program reported in this paper was to study the structural behavior of high strength SCC beams cast using third generation PCE and designed to fail in flexure, shear, or bond splitting. Accordingly, the behavior of SCC beams and control VC beams was compared. The two types of beams had identical geometrical, structural and concrete mix designs but were

made with different types of superplasticizers. This methodology distinguishes the current research from previously conducted research studies found in the literature review, and makes it significant. The objective of the study stems from the need to test the hypothesis that the high fluidity of SCC could adversely affect the shear strength of SCC members and the bond strength of bars anchored in full-scale structural members. The hypothesis is partially supported by the reported shear studies in the literature and the fact that the previous studies, bond and shear, included different constituents between the SCC and the normal concrete mixes.

4. Materials and Methods

4.1 Variables and Specimen Design

Twelve beams were tested as identified in Table 1. The beams are named according to their mode of failure: flexural beams, shear beams or bond beams. For each of the three modes, four beams were tested with two identical replicates made of SCC or VC. Replicates were used to validate the test results. The comparison of the beam specimen behavior was conducted in terms of two variables. The first variable is the type of concrete used in the placement of the tested beams: SCC denotes that third generation (PCE) was incorporated in the production of the concrete mix, while VC indicates that the concrete mix was made using second generation (SNF) superplasticizer. The second variable is the mode of failure of the tested beam (flexural, shear or bond splitting).

Accordingly, the beams are identified by a three part notation system. The first term indicates the type of concrete mix used in the casting of the beam (SCC or VC). The second term specifies the preset mode of failure (F for flexure, SH for shear, and B for bond splitting). The third term designates the listing number of the two replicates (B1 or B2).

The flexural beams were properly designed and reinforced to avoid shear failure before steel yielding. The shear beams were under-reinforced in shear to prompt brittle shear failure. The bond beams had their bottom tensile bars spliced at midspan, the lap length was chosen to be the minimum recommended by the ACI building code to avoid the yielding of the bottom bars and to ensure a concrete splitting mode of failure in the splice region. Longitudinal and cross sectional details are shown in Figs. 1, 2 and 3.

The beam specimen was 2,000 mm long with a distance of 1,800 mm between supports. The width of the beam was 200 mm and the depth was 300 mm.

4.2 Constituent Materials

4.2.1 Concrete

The twelve beams were cast at a ready-mix plant. With the exception of the type of superplasticizer, the mix proportions were identical and designed to produce a nominal concrete compressive strength of 60 MPa.

The consistency of the VC mix was adjusted using a second generation (SNF) superplasticizer while self-consolidation characteristics of SCC were provided by a third generation (PCE) superplasticizer.

The proportions of concrete mixes, designed according to the UCL method (Domone 2009), are presented in Table 2. A bulk dosage of 1.6 % was used as the optimal second or third generation superplasticizer to produce a cohesive high workability concrete mix as was proven in the earlier phases of the research. Table 3 displays the fresh properties of the concrete mixes used to cast the reinforced concrete beams. All twelve beams were cast on the same day. One batch was used for the VC beams and another batch for the SCC beams.

Standard 150 × 300 mm cylinders taken from the SCC and VC concrete batches produced at the ready-mix plant, were cast and tested to determine the concrete compressive

Table 1 Variables of the test program.

Beam type	Beam notation	Concrete mix	Mode of failure
Flexural beams	SCC-F-B1	SCC	Flexure
	SCC-F-B2	SCC	Flexure
	VC-F-B1	VC	Flexure
	VC-F-B2	VC	Flexure
Shear beams	SCC-SH-B1	SCC	Shear
	SCC-SH-B2	SCC	Shear
	VC-SH-B1	VC	Shear
	VC-SH-B2	VC	Shear
Bond beams	SCC-B-B1	SCC	Bond splitting
	SCC-B-B2	SCC	Bond splitting
	VC-B-B1	VC	Bond splitting
	VC-B-B2	VC	Bond splitting

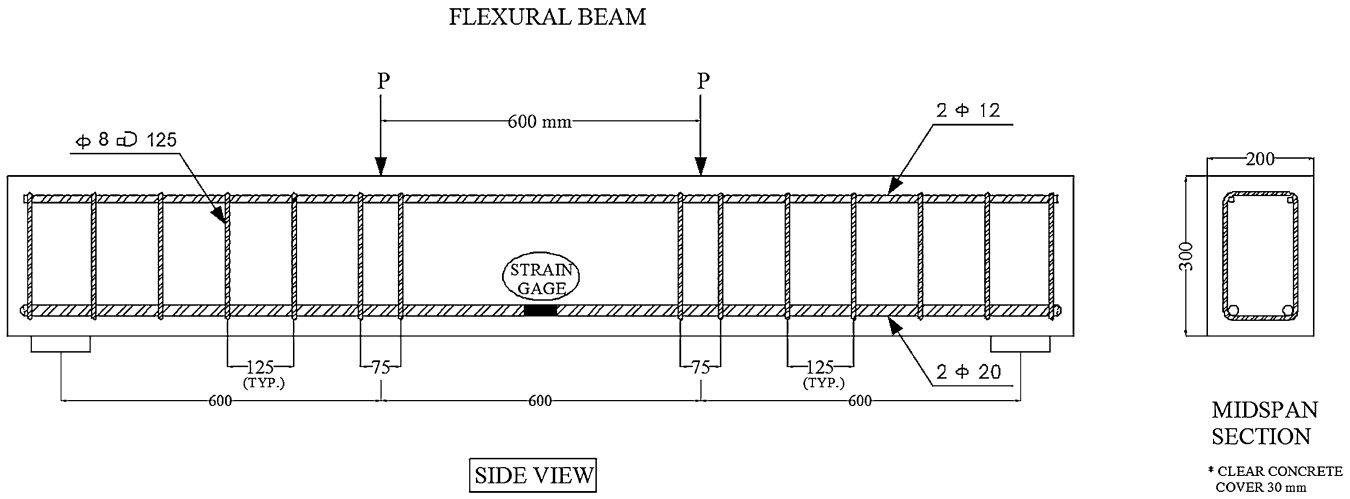

Fig. 1 Flexural beams; all dimensions are in mm.

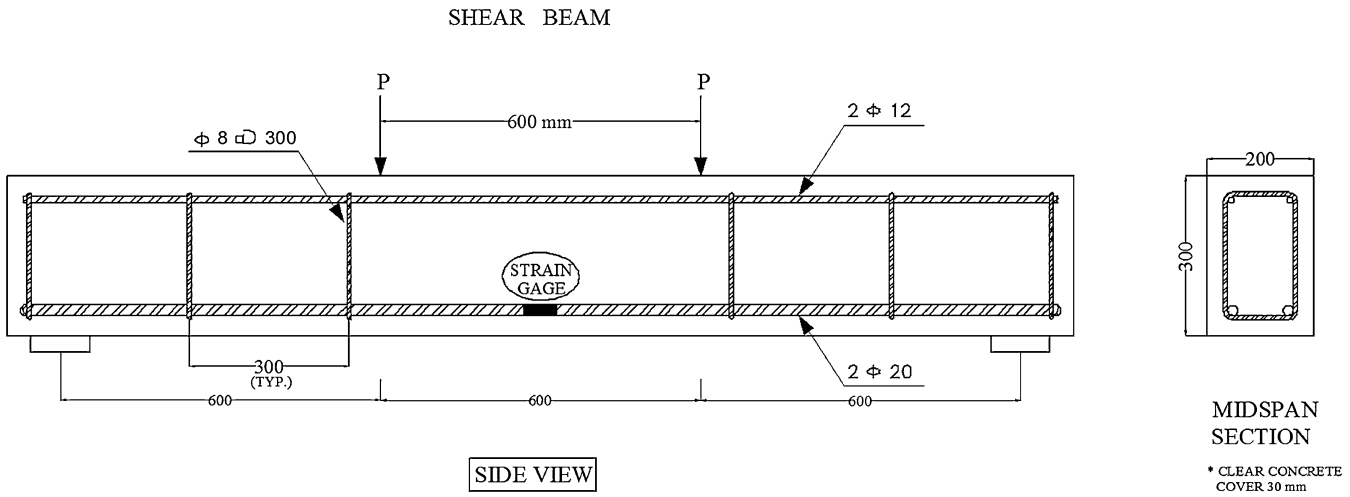

Fig. 2 Shear beams; all dimensions are in mm.

strength f'_c, the tensile strength f_t, and the modulus of elasticity E_c.

Standard plain concrete beams were also prepared to determine the flexural strength or modulus of rupture f_r. Average results corresponding to the VC and SCC beams are listed in Table 4. The cross section of a typical SCC plain beam, shown in Fig. 4, displays the uniformity of the aggregate distribution ensured by the proper cohesion of the high consistency SCC mix produced with a bulk PCE dosage of 1.6 %.

4.2.2 Steel Reinforcement

The reinforcement of each beam consisted of two longitudinal 20 mm reinforcing bars located at the bottom tension side and two 12 mm reinforcing bars at the top compression side. Stirrups, 8 mm in diameter, were provided in the critical shear regions. All bars were Grade 60 satisfying ASTM A615M (2012). Samples for each bar-size were tested to determine the yield, ultimate strengths and the modulus of elasticity. Values are shown in Table 5. In each beam, the top and bottom bars were cut to ensure a 30 mm clear concrete cover at the ends of the beam. In the bond beams, the bottom reinforcing bars were spliced 305 mm at the midspan.

The shear reinforcement consisting of closed hoop stirrups were also dimensioned taking into account a design concrete cover of 30 mm on the 4 sides. With reference to ACI 318-11 (2011), a minimum inside bend diameter of 4 d_b was adopted for the stirrups with a minimum extension length of 50 mm at the free end of the bar, equivalent to 6 d_b.

In order to monitor the strain in the steel bars during testing, each beam had one strain gage sealed to each of the two bottom reinforcing bars. In the flexural and shear beams, the strain gages were located at the middle of the bars, whereas in the bond beams the strain gages were placed at the end of the splice length.

4.2.3 Admixtures

4.2.3.1 Sulphonated Naphtalene Formaldehyde-Based Superplasticizer (Dransfield 2003) The sulphonated naphtalene formaldehyde superplasticizer is a Type F admixture manufactured in accordance with ASTM C494 standard. After being extracted from petroleum or coal tar, naphtalene, composed of a fused pair of benzene rings, undergoes sulphonation then, polymerization until the final structure takes the shape shown on Fig. 5. When the superplasticizer is mixed with water, Na^+ dissociates from

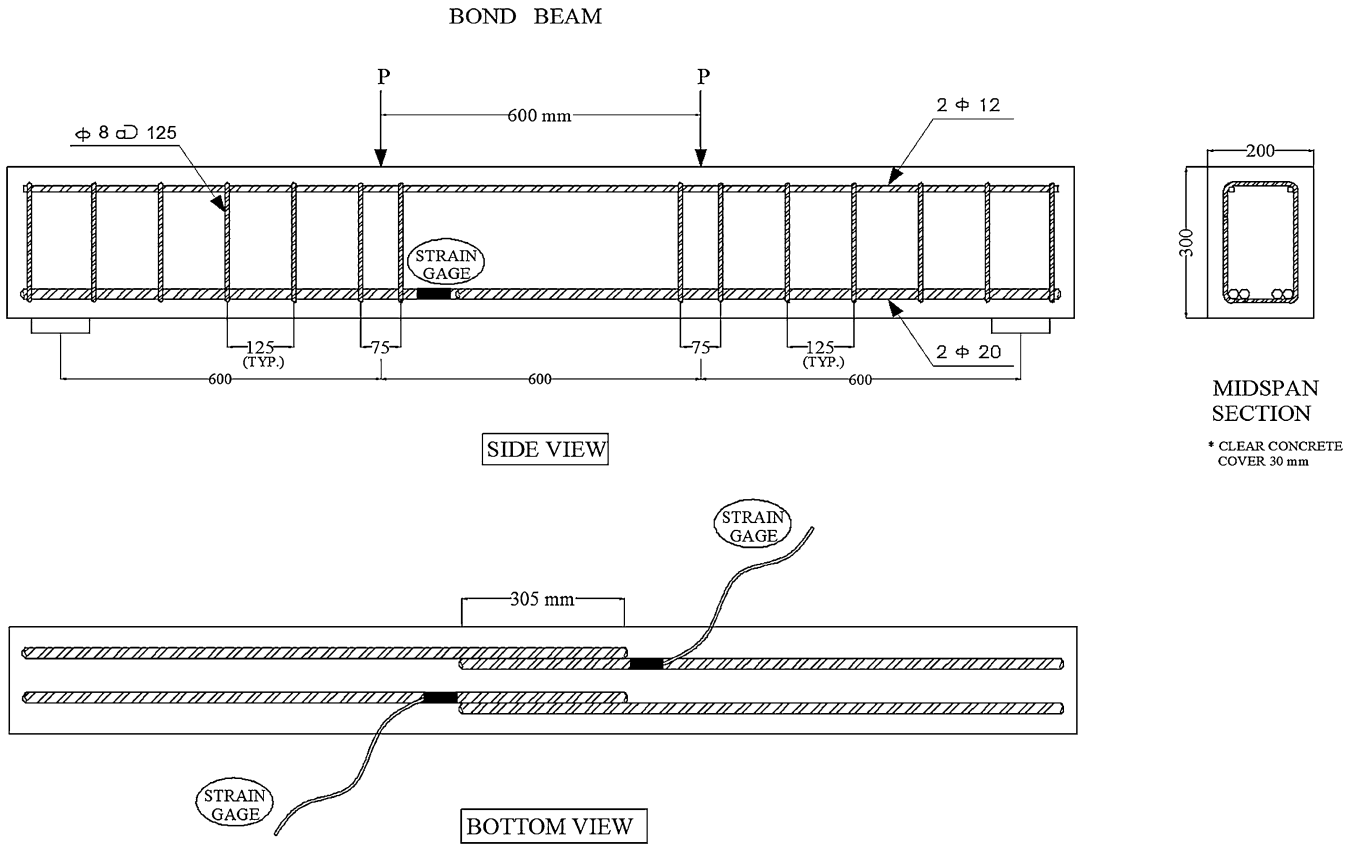

Fig. 3 Bond beams; all dimensions are in mm.

Table 2 Concrete mix proportions.

Constituent materials	Mix proportioning
Cement (kg/m^3)	575
Natural sand 0–1.18 mm (kg/m^3)	453
Crushed sand 0–4 mm (kg/m^3)	371
Coarse aggregates 4–10 mm (kg/m^3)	807
Water (kg/m^3)	194
Bulk dosage of SNF or PCE superplasticizer by weight of cement (%)	1.6 %
SNF or PCE based superplasticizer (kg/m^3)	9.2

Table 3 Fresh concrete properties.

Concrete mix type	% Bulk SP	Slump (mm)	Spread flow test (mm)
VC	1.60	210	–
SCC	1.60	–	790

Table 4 Average hardened concrete properties.

Strength (MPa)	SCC	Theoretical	VC	Theoretical
$f_c^{'}$	62.4	62.4	57.9	57.9
E_c	35,133	35,624	33,103	34,746
f_t	4.3	4.7	3.8	4.5
f_r	6.0	4.9–7.8	5.1	4.7–7.5
f_t/f_r	72 %	–	75 %	–

Fig. 4 Aggregate distribution in a typical SCC sample plain beam (150 × 150 × 520 mm).

SO_3^- leaving a negatively charged molecule that will adsorb onto the positively charged cement particle. The negative charge on the admixture will be partially used to attach the superplasticizer on the cement while the remaining free negative charges will be used to repulse the neighboring identically charged particles ensuring by this way the dispersion of cement. The electrostatic repulsion mechanism of action is demonstrated in Fig. 6.

4.2.3.2 Polycarboxylate Ethers (PCE) Based Superplasticizer: Third Generation SP (Dransfield 2003)

Polycarboxylate ethers are comb-like polymers consisting of the backbone polymer attached to numerous carboxylate groups and polyether chains. The chemical structure of the superplasticizer can be tailored based on the required admixture performance. Therefore, polycarboxylate ethers form a wide family of chemical products created to meet particular application requirements. The PCE admixture mentioned in this research was specifically manufactured for usage in ready mix plants in accordance to BS EN 934-2 standard. Figure 7 displays the chemical structure of one type of PCE admixtures. Similarly to SNF superplasticizers, when in contact with water, the sodium ion separates from the polycarboxylate ether polymer to leave behind a negatively charged molecule that will adsorb onto the cement particle. The polyether chains directed outward from the cement particle will be the one responsible for keeping a distance between the adjacent cement elements while

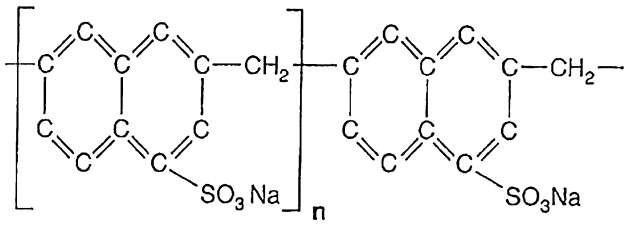

Fig. 5 Chemical structure of sulphonated naphtalene formaldehyde based superplasticizer.

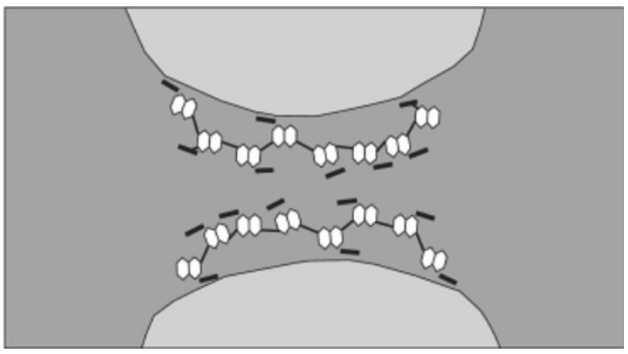

Fig. 6 Dispersion mechanism of SNF superplasticizer.

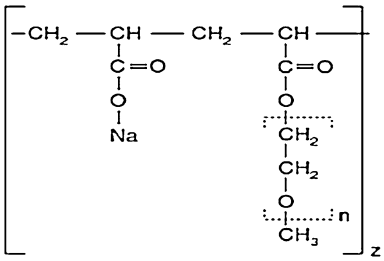

Fig. 7 Chemical structure of polycarboxylate ether based superplasticizer.

avoiding to become entangled with the neighboring chains following a mechanism recognized as the steric stabilization. Figure 8 clarifies the steric dispersing action.

4.3 Testing Procedure

The reinforced concrete beams were tested using an MTS (Material Testing System) closed loop servo-hydraulic machine with a dynamic actuator having a capacity of 1,000 kN. The span between the centerlines of the supports was taken to be 1,800 mm. The beams were tested in positive bending. The loading system was designed to produce a constant moment region (zero shear) in the middle of the

Table 5 Yield and ultimate strengths of longitudinal and transverse reinforcing bars.

	Rebar size	f_y (MPa)	f_u (MPa)	E_s (MPa)
Bottom reinforcement	2 Φ 20	632.0	743.0	200,000.0
Top reinforcement	2 Φ 12	557.0	667.0	290,000.0
Shear reinforcement	2 Φ 8	569.0	661.0	220,000.0

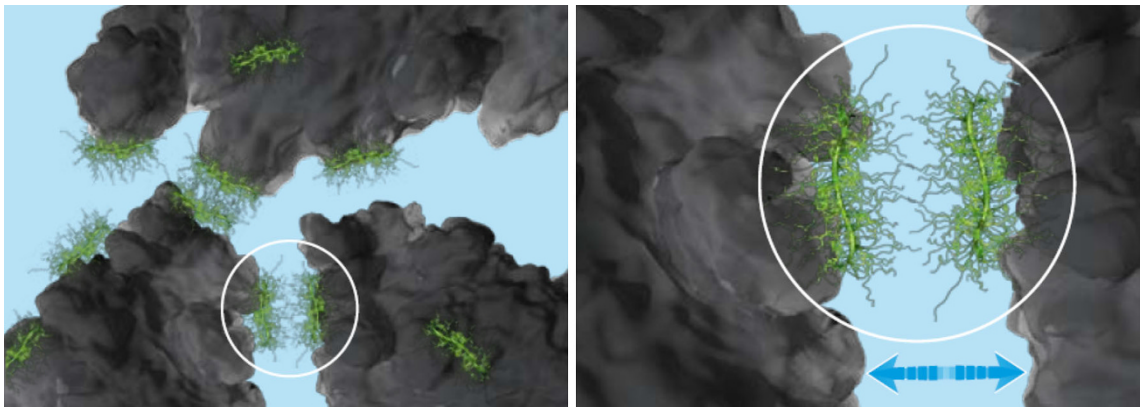

Fig. 8 Steric hindrance dispersion mechanism of PCE superplasticizer.

beam specimen. Two concentrated loads were applied continuously at a distance from the two supports equivalent to one third of the span length (600 mm). A steel plate was placed under each point load to distribute the load evenly over the 200 mm beam width. The vertical deflection was monitored at midspan using an LVDT sensor. The two strain gages mounted on the bottom tensile reinforcing bars were connected to a computer system to record the steel elongations inside the concrete. The loads were applied in increments of 10 kN until failure. At each load increment, crack width readings were taken using a crack comparator. In the flexural and shear beams, cracks that have initiated below the two concentrated loads and at midspan were observed. In the bond beams, cracks located at the end of the lap splices were also checked. In all beams, the propagation and widening of the shear cracks were examined attentively. An actual view of the testing setup of beam specimen is shown in Fig. 9. A schematic is also shown in Fig. 10.

5. Analysis of Test Results

Summary of the test results of all twelve beams is presented in Table 6. The listed data includes the ultimate load reached and the corresponding midspan deflection.

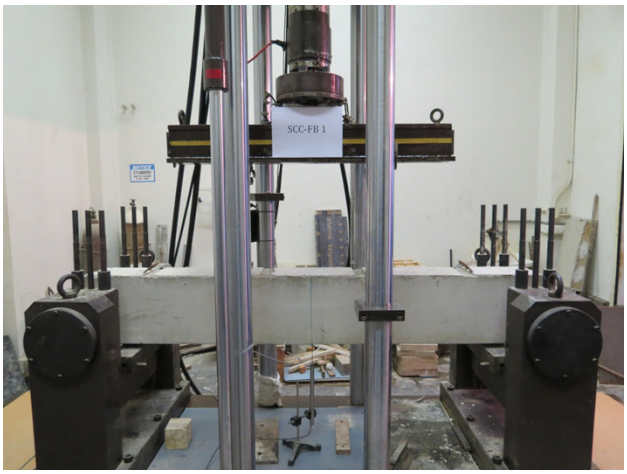

Fig. 9 View of the testing setup of a beam specimen.

5.1 Hardened Concrete Properties

The following sections present the equations for the modulus of elasticity, the splitting tensile strength and the modulus of rupture that were found to best represent the experimental outcomes.

5.1.1 Modulus of Elasticity

The theoretical modulus of elasticity was computed using Eq. (1). To avoid underestimating the modulus of elasticity of high strength concrete, the best fit theoretical equation was found to be a function of the cube root of the compressive strength rather than the square root. Among all the equations listed in the ACI Report on High strength Concrete (ACI Committee 363R 2010), the most representative equation for SCC mixes was the one recommended by the FIP-CEB (1990) state-of-the-art-report that provides a close estimation on the elasticity modulus. Under ultimate loading conditions, the failure in high strength concrete is induced by the splitting of coarse aggregates rather than the development of unstable microcracking in mortar. Therefore, as declared in the report (ACI Committee 363R 2010), the modulus of elasticity of high strength concrete is highly dependent on the coarse aggregate volumes and characteristics. The coarse aggregate constituent in the SCC and VC mixes had an MSA of 10 mm what might have caused the deviation of the experimental results from the theoretical predicted values. It is worth noting that this deviation was more pronounced in VC mixes.

$$E_c = 21,500\alpha_\beta [f_{cm}/10]^{1/3} \quad \text{(in MPa)} \tag{1}$$

where $\alpha_\beta = 0.9$ for limestone aggregates

5.1.2 Splitting Tensile Strength

The ACI equation (Eq. 2) presented in the ACI Report on High strength Concrete (ACI Committee 363R 2010) has demonstrated to be reliable in the determination of the theoretical splitting tensile strength of high strength concrete, Carrasquillo et al. (ACI Committee 363R 2010). developed Eq. (1) that was adopted in this research.

$$f_{ct} = 0.56\sqrt{f_c'} \quad \text{(in MPa)} \tag{2}$$

The findings of Dewar (1964), stating that the splitting tensile strength can reach 70 % of the flexural strength at

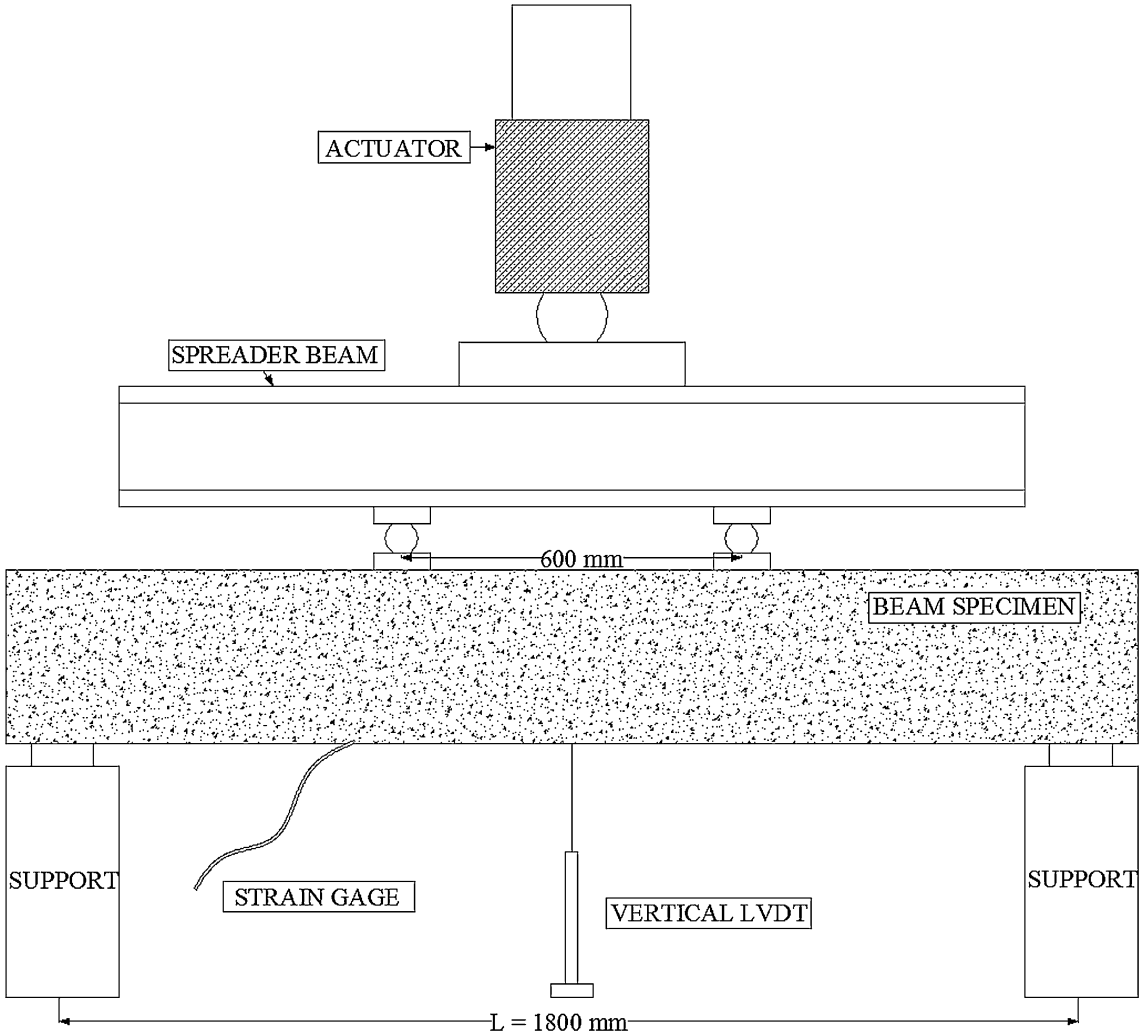

Fig. 10 Schematic of the test setup.

Table 6 Ultimate loads and maximum deflections at failure.

Beam type	Beam notation	P_{max} (kN)	Δ_{max} (mm)
Flexural beams	SCC-F-B1	158.4	15.5
	SCC-F-B2	149.6	19.4
	VC-F-B1	154.8	13.5
	VC-F-B2	157.2	30.2
Shear beams	SCC-SH-B1	132.3	14.9
	SCC-SH-B2	107.4	8.2
	VC-SH-B1	111.5	7.8
	VC-SH-B2	127.9	11.2
Bond beams	SCC-B-B1	93.1	6.6
	SCC-B-B2	87.2	5.3
	VC-B-B1	87.7	9.9
	VC-B-B2	90.5	8.0

28 days, were reflected in this research where the reported tensile strengths attained 70–75 % of the flexural strength respectively in SCC and VC mixes.

5.1.3 Modulus of Rupture

Previous research has reported that the modulus of rupture of normal density high strength concrete falls in the range specified by Eq. (3), where the lower bound was recommended by ACI 318-11 (ACI Committee 318 2011) for normal density concrete, while the upper bound was developed by Carrasquillo (ACI Committee 363R 2010) in 1989.

$$f_r = 0.62\sqrt{f_c'} \text{ to } 0.94\sqrt{f_c'} \quad \text{(in MPa)} \tag{3}$$

The experimental modulus of rupture for the SCC beams appeared to fall in the middle range of the expression presented by Eq. (3) and that can be defined by the following Eq. (4).

$$f_r = 0.76\sqrt{f_c'} \quad \text{(in MPa)} \tag{4}$$

The experimental modulus of rupture for the VC beams appeared to satisfy Eq. (5).

$$f_r = 0.67\sqrt{f_c'} \quad \text{(in MPa)} \tag{5}$$

5.2 Bond Strength

The proper performance of reinforced concrete members in flexure or direct tension comes as a result of adequate force transfer between reinforcing bars and concrete. In their studies on the behavior of full-size reinforced concrete elements in bond splitting modes of failure, researchers opted to use splice specimens that appeared to be effective in providing realistic experimental data. Accordingly, four beam specimens were cast to test and compare the bond strength of steel reinforcement in SCC beams.

Results of the tests on bond beams are listed in Table 7. The results include the ultimate load at bond splitting failure, the number of cracks and the maximum flexural crack width at the end of the splice region. The crack widths listed in Table 7 and the cracked beam sketches, associated with SCC and VC bond beams displayed in Figs. 11–20 revealed similar cracking patterns of replicate SCC and VC beams.

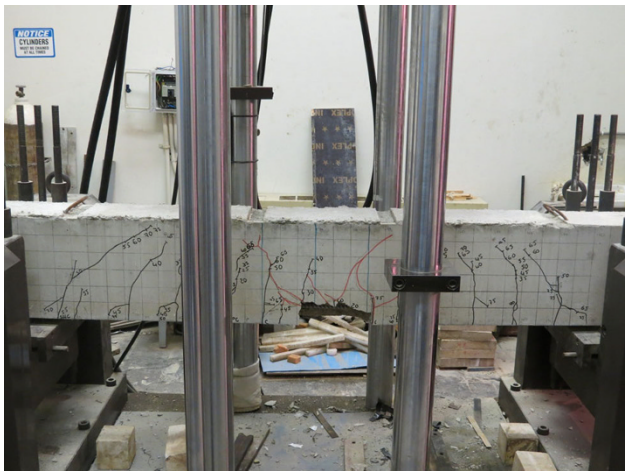

Fig. 11 Cracked bond beam (SCC-B-B2).

Fig. 12 Close view of the crack pattern and mode of failure associated with the bond beam (SCC-B-B2).

Figure 21 displays the response of bond beams to equal load increments. The load deflection curves of SCC-B-B1, SCC-B-B2, VC-B-B1 and VC-B-B2 demonstrated similar stiffness characteristics. The average load resulting in the bond splitting failure was approximately 90.2 kN in reinforced SCC beams and 89.1 kN in VC beams. This experimental result has proven compliance with the equation suggested by ACI committee 408 (2003) ($P_{SCC} = 75.7$ kN and $P_{VC} = 74.3$ kN) and Darwin et al. (ACI Committee 408R 2003). ($P_{SCC} = 70.7$ kN and $P_{VC} = 69.4$ kN) that

Table 7 Test results of bond beams.

Specimen notation	SCC-B-B1	SCC-B-B2	VC-B-B1	VC-B-B2
P at bond splitting failure (kN)	93	87	88	91
Number of cracks	14	14	15	15
Max. flexural crack width at splice end (mm)	0.20	0.20	0.20	0.20

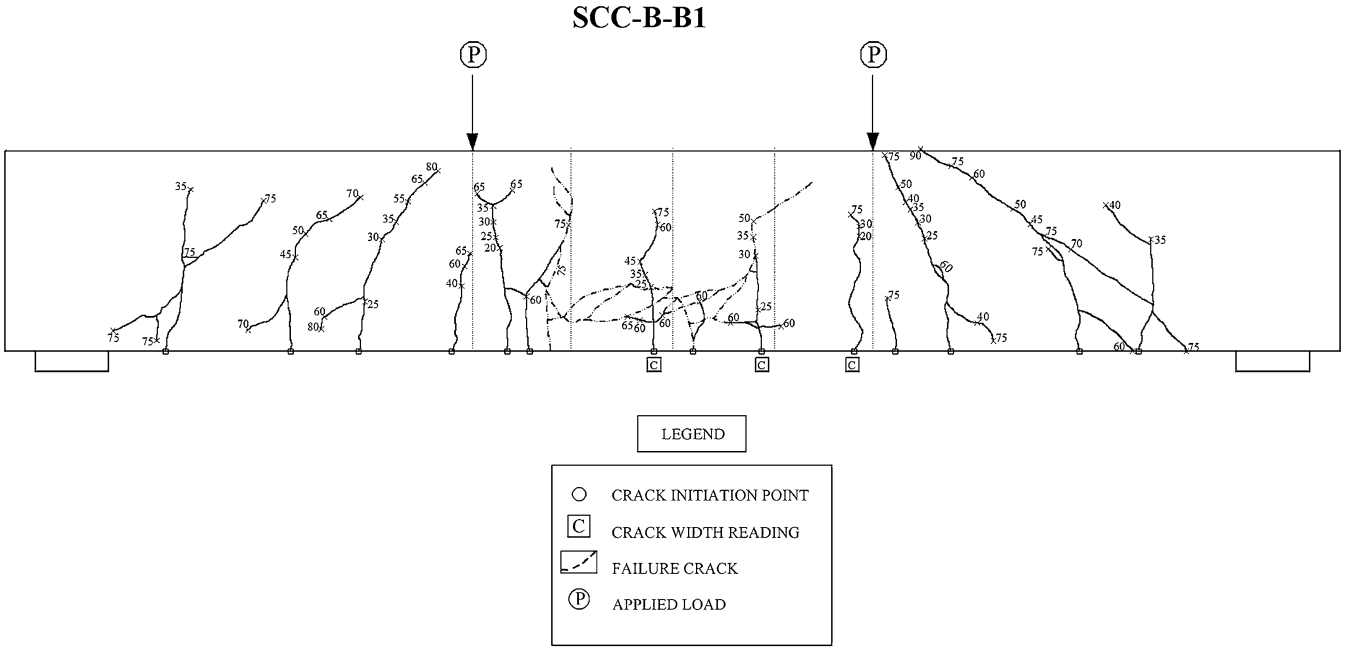

Fig. 13 Side view of the crack pattern and mode of failure associated with beam (SCC-B-B1).

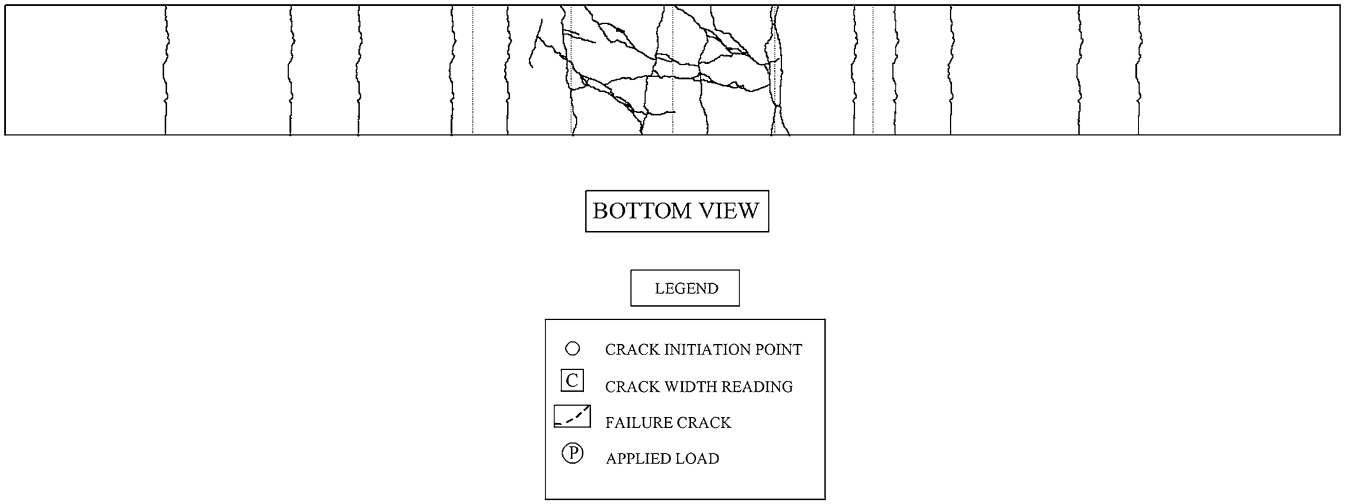

Fig. 14 Bottom view of the crack pattern and mode of failure associated with beam (SCC-B-B1).

provide conservative predictions on the bond strength of SCC and VC beams with factors of safety ranging from 1.2 to 1.3. The equation proposed by Esfahani and Rangan (ACI Committee 408R 2003) for high strength concrete overestimates the capacity of reinforced SCC and VC beams ($P_{SCC} = 107.1$ kN and $P_{VC} = 103.2$ kN). The theoretical equations considering the contribution of transverse reinforcement in the transfer of bond stresses were disregarded.

The test results of the bond beams indicate that the high fluidity characteristics of SCC mixes have no impact on the bond characteristics of reinforcing bars, a statement that refutes the hypothesis presented earlier in this paper.

5.3 Shear Strength

The shear strength of SCC is designated by the ultimate load that triggered the appearance of the first diagonal crack and was evaluated through the close monitoring of the development of this crack. Since the concrete shear strength in beams is dependent on the tensile characteristics of concrete and is independent of the area of transverse reinforcement allocated for a concrete section, the concrete shear strength results of the flexure and shear beams were considered. In the analysis of the test results, the experimental values were compared to the theoretical estimation of the concrete strength in shear. The maximum shear capacity carried by concrete was computed using Eqs. (11-5) of Sect. 11.2.2.1 of the ACI Building Code ACI 318-11 (2011). The ACI equation for the shear strength considers the effect of the longitudinal reinforcement and the applied moment on the shear resistance of reinforced concrete beams.

Test results of the shear beams are listed in Table 8. The results include the load at first diagonal crack and the ultimate shear load at failure. Also listed in Table 8, are the number of cracks and the maximum shear crack width. The crack patterns of SCC and VC shear beams beam are shown in Figs. 22–25.

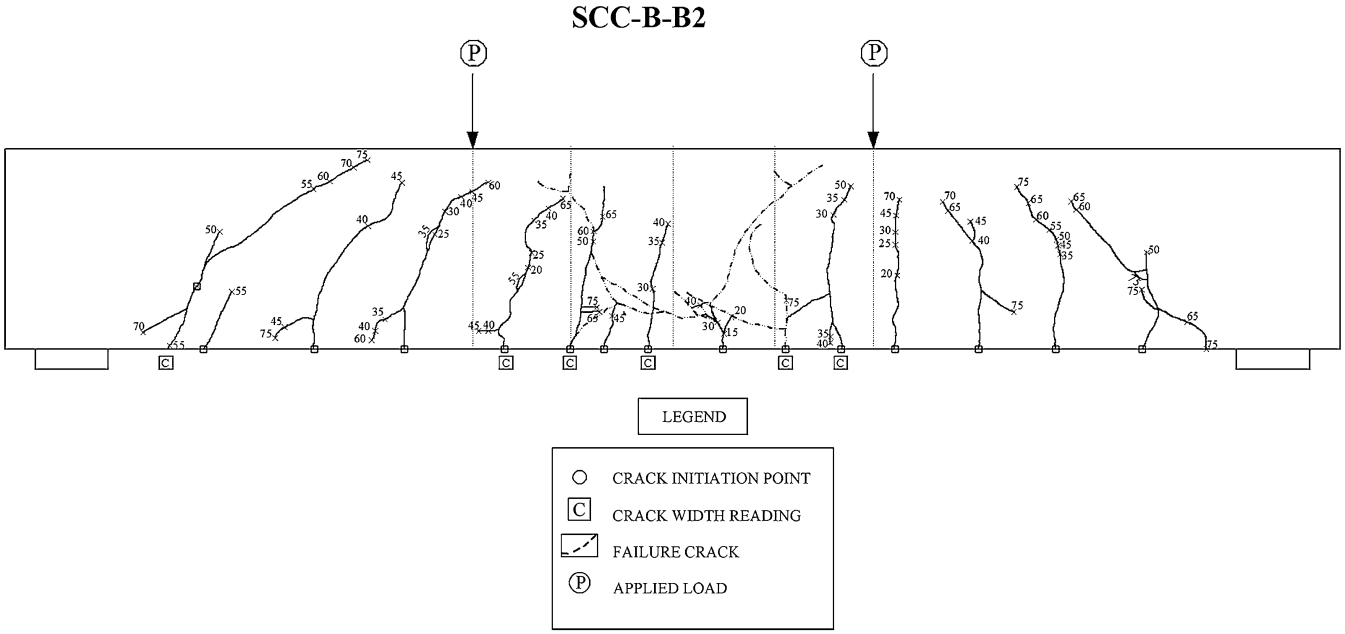

Fig. 15 Side view of the crack pattern and mode of failure associated with beam (SCC-B-B2).

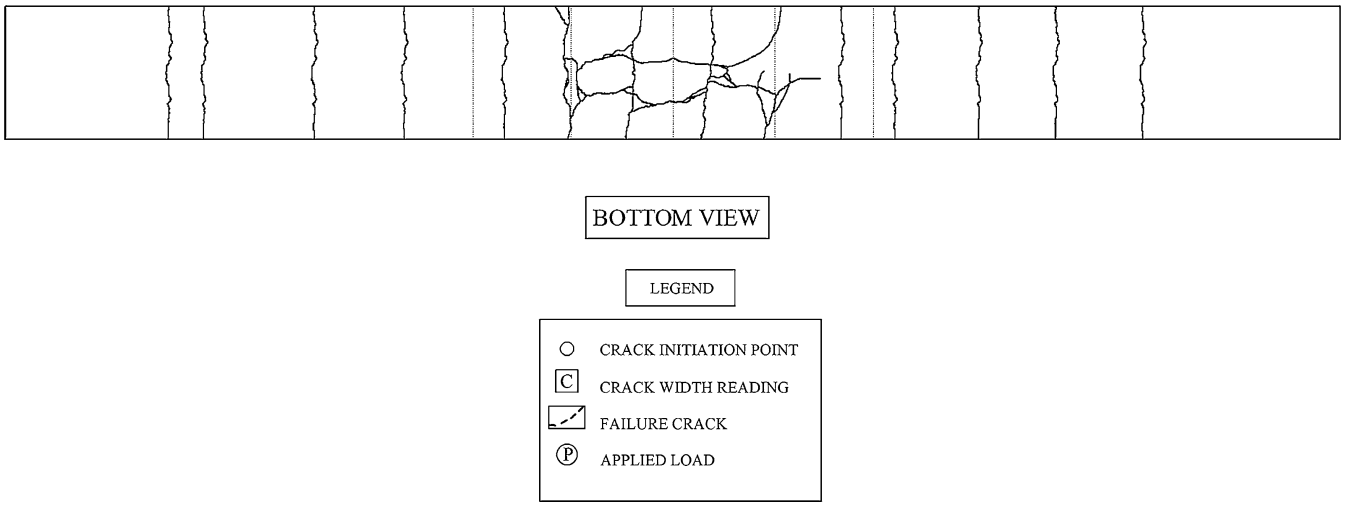

Fig. 16 Bottom view of the crack pattern and mode of failure associated with beam (SCC-B-B2).

The experimental results revealed an average concrete shear capacity of 50 kN in SCC beams and 42.5 kN in VC beams compared to a theoretical concrete shear load of 55.5 kN for SCC beams and 53.8 kN for VC beams. A reduction factor ϕ of 0.75 was used in the computation of all the theoretical concrete shear capacities.

Considering identical mix designs for SCC and VC, SCC demonstrated better shear resistance than its VC counterpart. Consequently, the high consistency of self-consolidating concrete has little effect on the concrete capacity in shear.

On the other hand, both SCC and VC beams have shown a concrete capacity that is lower than the nominal capacity computed using Eq. (11-5) of ACI 318-11 (2011). The ACI report on high strength concrete (ACI 363R 2010) states that with increasing concrete compressive strength, the actual concrete contribution in the shear resistance reveals lower values than the ones predicted through the more complex ACI equation for V_c due to the reduction in the aggregate interlock for HSC.

In the case where the concrete shear resistance was computed using the simplified Eq. (11-3) of the ACI 318-11 (2011), the theoretical concrete shear capacity of SCC becomes 50 kN compared to 48.2 kN for VC beams. The simplified equation has proven to be the best fit equation for the estimation of the SCC shear capacity and can be considered as reliable in the simulation of the behavior of SCC beams in shear. The adoption of Eq. (11-3) appears to conservatively cover the effect of the reduction in the aggregate interlock in SCC beams through providing theoretical estimations that are equal to the experimental values. In contrast, this same equation is not representative of the behavior of VC beams.

The loads at ultimate shear failure for the four shear beams, consisting of the combined concrete and transverse reinforcement shear capacity, are listed in Table 8. The load–deflection curves shown in Fig. 26 indicate similar load–deflection history for the VC and SCC beams.

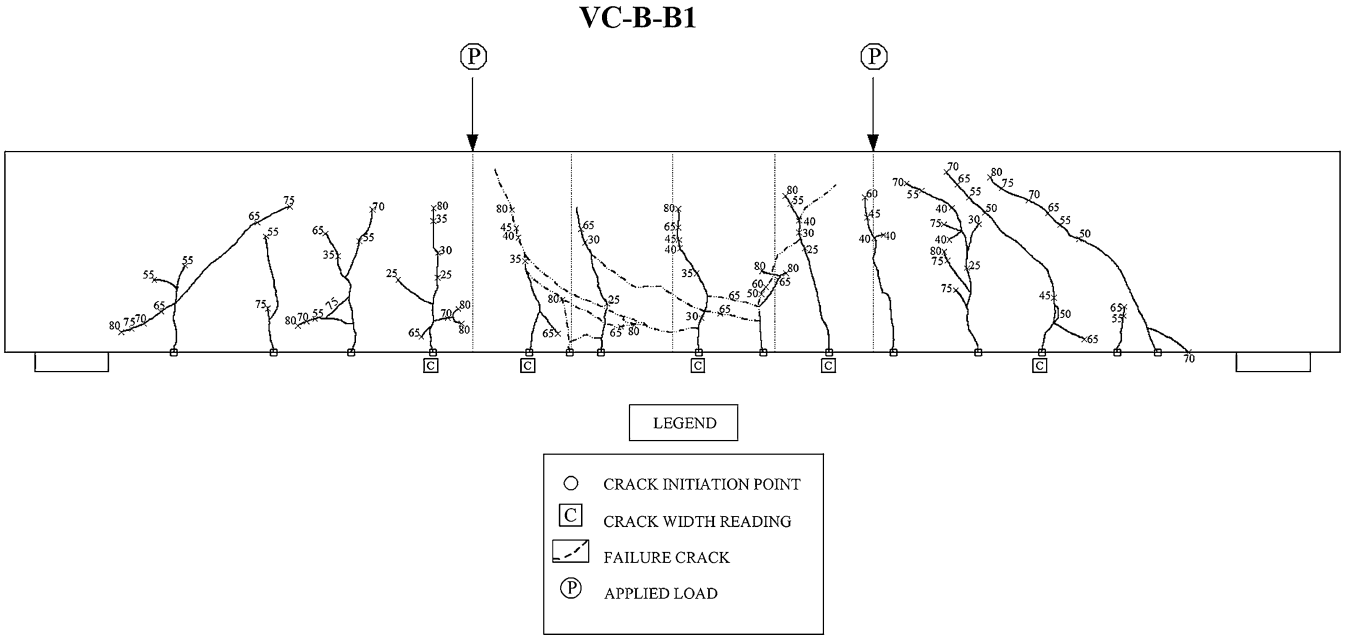

Fig. 17 Side view of the crack pattern and mode of failure associated with beam (VC-B-B1).

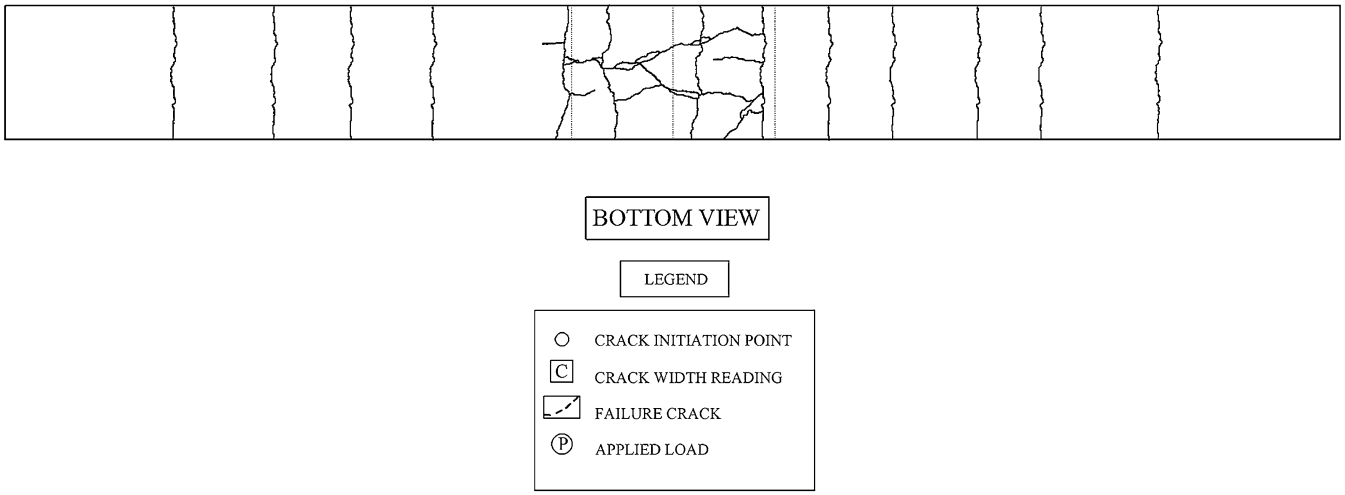

Fig. 18 Bottom view of the crack pattern and mode of failure associated with beam (VC-B-B1).

The results of the shear failure of SCC and VC beams revealed an equal average ultimate shear capacity of approximately 120 kN in both beam types. The theoretical ultimate shear capacity was found to be equivalent to 93 kN in SCC beams and 91 kN in VC beams.

Crack patterns were very similar for replicate identical shear beams and were very similar for the VC and SCC beams. The diagonal crack widths constant for identical shear and flexural beams indicate the consistency of the test results.

These outcomes refute the hypothesis statement declaring that the high consistency of SCC will negatively affect the shear strength of SCC members. Also, the effect of the aggregate interlock on the concrete shear capacity was found to be more pronounced in VC beams than its is in SCC beams. This difference can be associated to the enhanced hydration of cement and the improved cohesiveness of the concrete mix.

5.4 Flexural Strength

Test results of the flexural beams are listed in Table 9. The results include the load at first diagonal crack, the load at yielding, and the ultimate load at failure. Also listed in Table 9, are the number of cracks and the maximum width of flexural and shear cracks.

The cracked beam sketches corresponding to SCC and VC shear beams are shown in Figs. 27–30.

The number of cracks and the crack width measurements disclosed similar values for the VC and SCC beams.

The loads at yielding and at ultimate for the four flexural beams are listed in Table 9.

The average yielding load for the two replicate beams was similar for SCC ($P_y = 99.5$ kN) and VC ($P_y = 91.5$ kN).

It was noticeable that the flexural crack height was greater in the SCC and VC beams than it was predicted using cracked section analysis. According to the ACI report on high strength concrete (ACI Committee 363R 2010), this

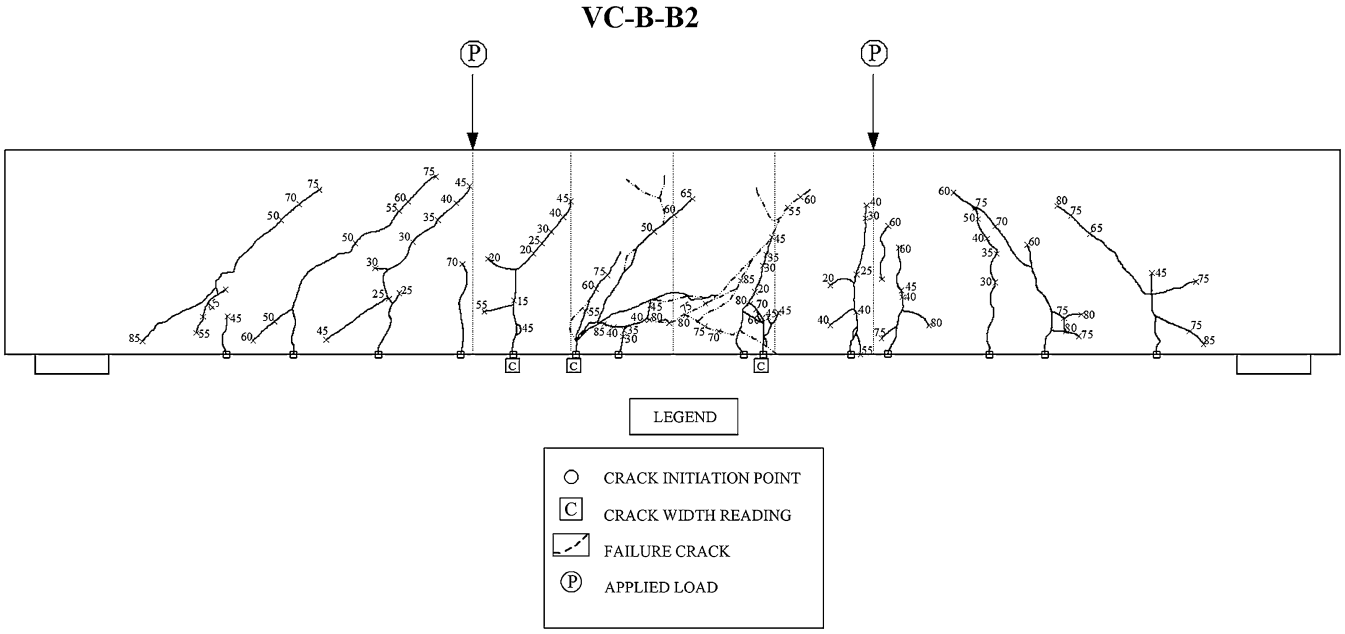

Fig. 19 Side view of the crack pattern and mode of failure associated with beam (VC-B-B2).

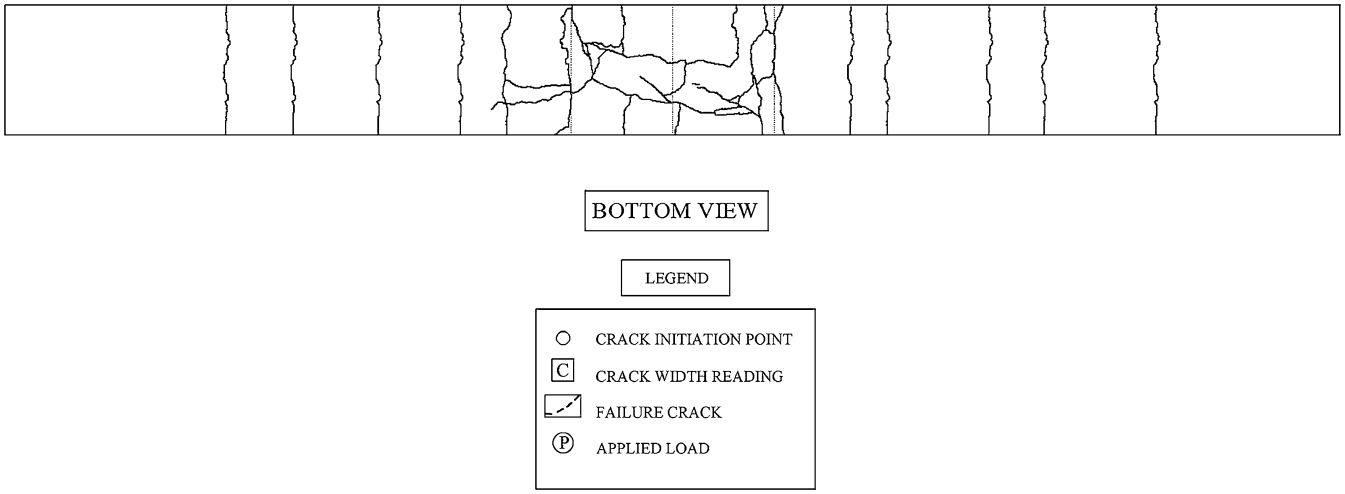

Fig. 20 Bottom view of the crack pattern and mode of failure associated with beam (VC-B-B2).

behavior can be foreseen in HSC beams where shallower compression zones are required to maintain equilibrium in flexure.

In reference to Eqs. (7)–(12) the ductility index was taken as the ratio of the deflection at failure to the deflection at the load producing reinforcement yielding.

Beyond the yield load, the flexural beams exhibited a shear mode of failure with an average maximum load in SCC beams of 154 and 156 kN in VC beams. These results confirm the findings of the shear beam experimentation analysis.

The load–deflection curves shown in Fig. 31, indicate very similar load–deflection history for the VC and SCC flexure beams. Based on the displacement ductility index, SCC and VC beams have also shown similar ductility in bending.

6. Conclusions

Twelve beam specimens were cast using either SCC or VC mixes. The beams were tested in flexure to investigate their structural behavior in three modes of failure: flexure, shear or bond splitting.

The concrete mixes were performed at a ready-mix plant with a bulk dosage of 1.6 % of second generation (SNF) superplasticizer and third generation (PCE) superplasticizer used respectively for the VC and SCC beams.

Using the MTS machine, the reinforced concrete beams were subjected to two concentrated loads located at one-third and two-third of the beam span length creating a constant moment region in the middle. The beam deflection, cracking and the tension reinforcement straining were closely monitored.

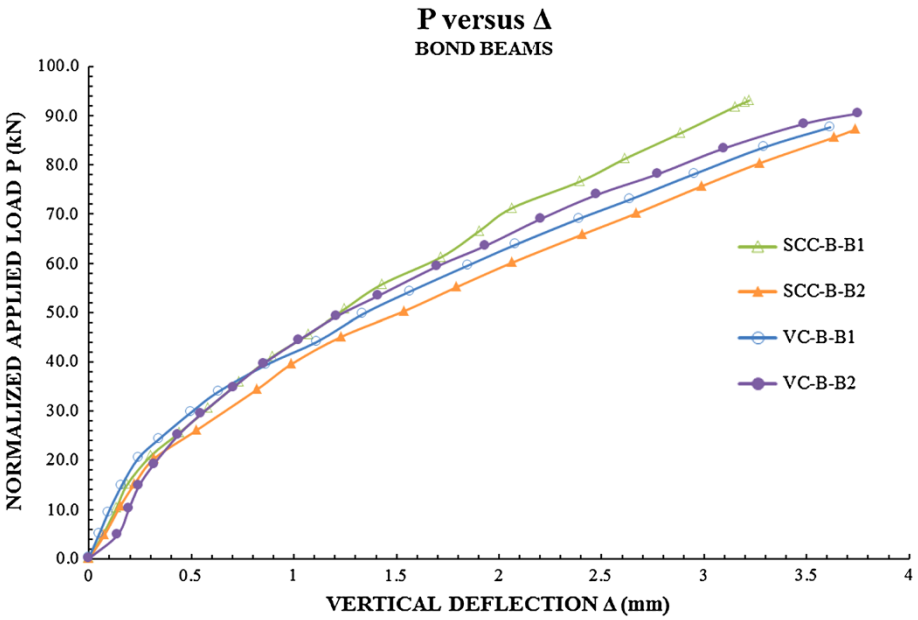

Fig. 21 Load–deflection curves of the bond beams.

Table 8 Test results of shear beams.

Specimen notation	SCC-SH-B1	SCC- SH-B2	VC-SH-B1	VC- SH-B2
P at first diagonal crack (kN)	50	50	40	45
P at ultimate shear failure (kN)	132	107	112	128
Theoretical ultimate shear (kN)	93	93	91	91
Number of cracks	10	12	10	13
Max. shear crack width (mm)	1.50	1.50	1.50	1.50

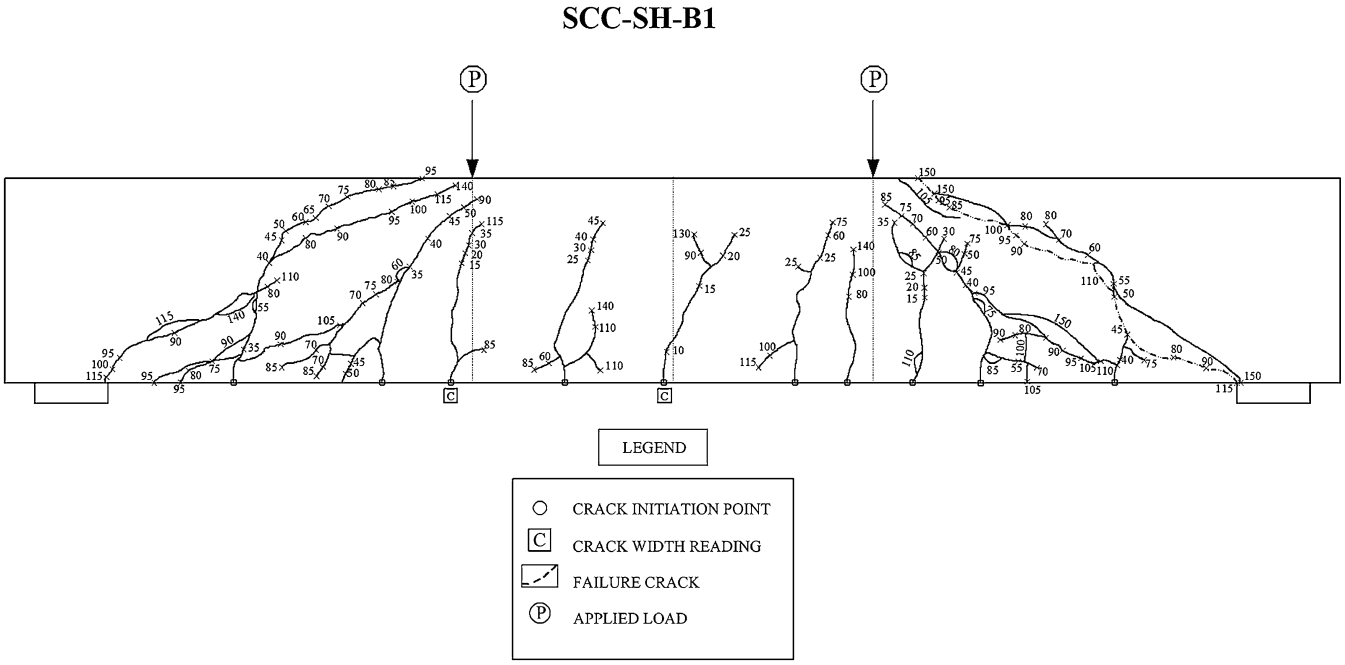

Fig. 22 Crack pattern and mode of failure associated with beam SCC-SH-B1.

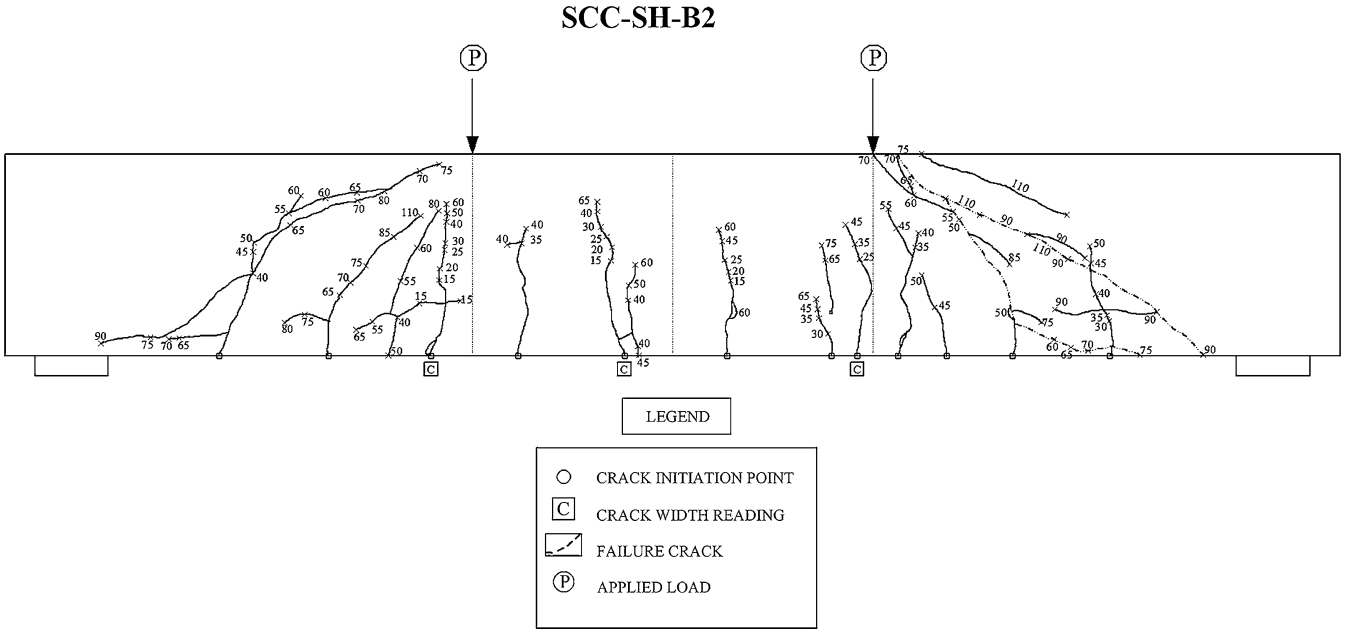

Fig. 23 Crack pattern and mode of failure associated with beam SCC-SH-B2.

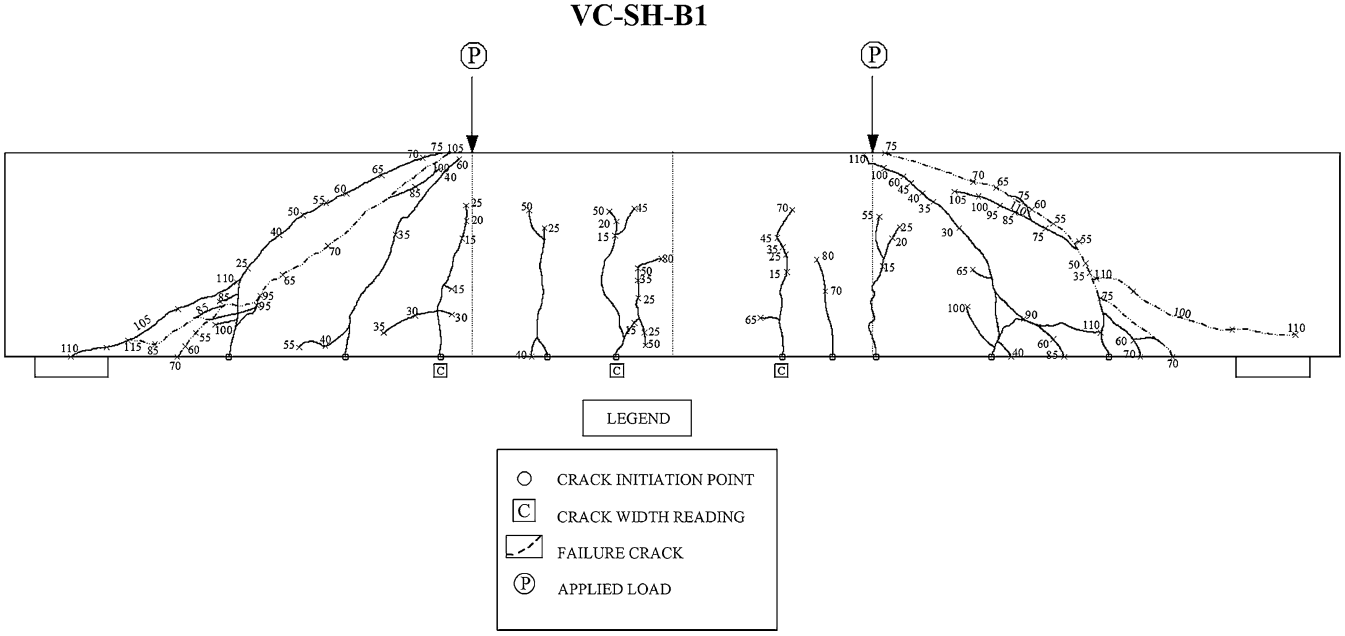

Fig. 24 Crack pattern and mode of failure associated with beam VC-SH-B1.

The dissimilarities in the experimental values between the SCC and the control VC beams were not significant. The analysis of the results revealed the following facts concerning the behavior of reinforced concrete beams cast using high consistency and vibrated concrete mixes having identical mix designs:

– Maximum crack widths were reported for the vertical cracks at midspan, at splice ends and under the two concentrated applied loads. As for the diagonal cracks, the maximum crack widths were measured at the supports in the flexure, shear and bond beams. The experimentations on flexure, shear, and bond beams cast using SCC and VC revealed similar cracking patterns and demonstrated consistent beam responses to load increments.
– The average splitting load failure of the bond beams appeared to be the same in SCC and VC beams which

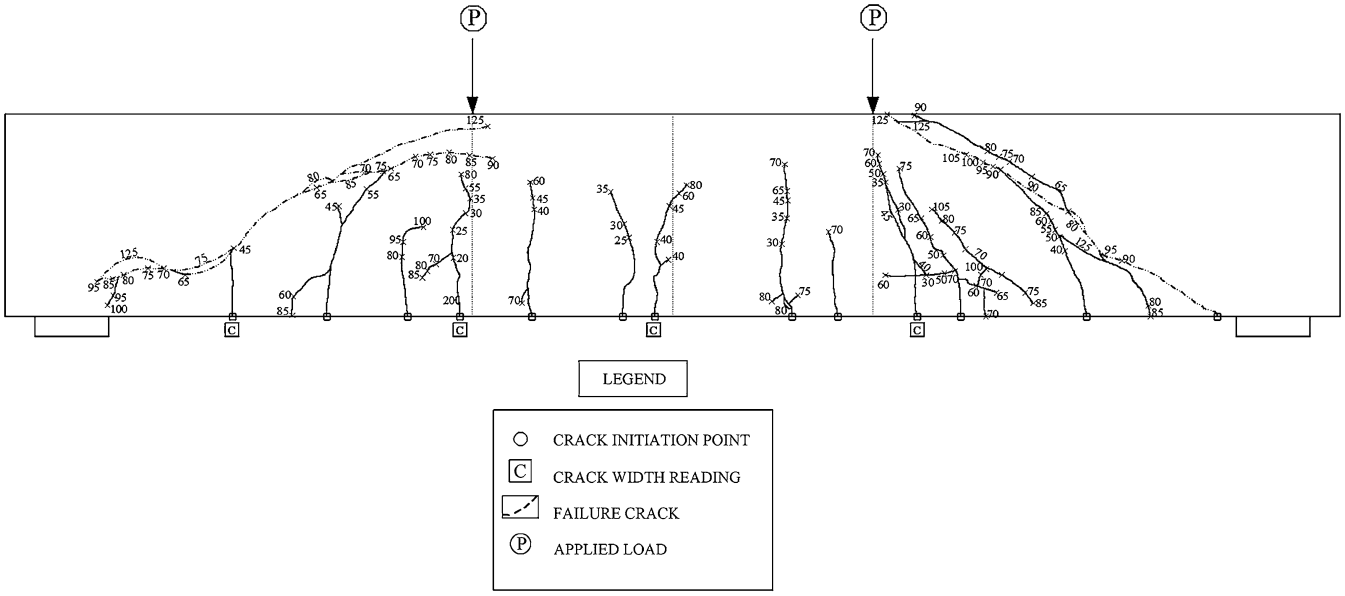

Fig. 25 Crack pattern and mode of failure associated with beam VC-SH-B1.

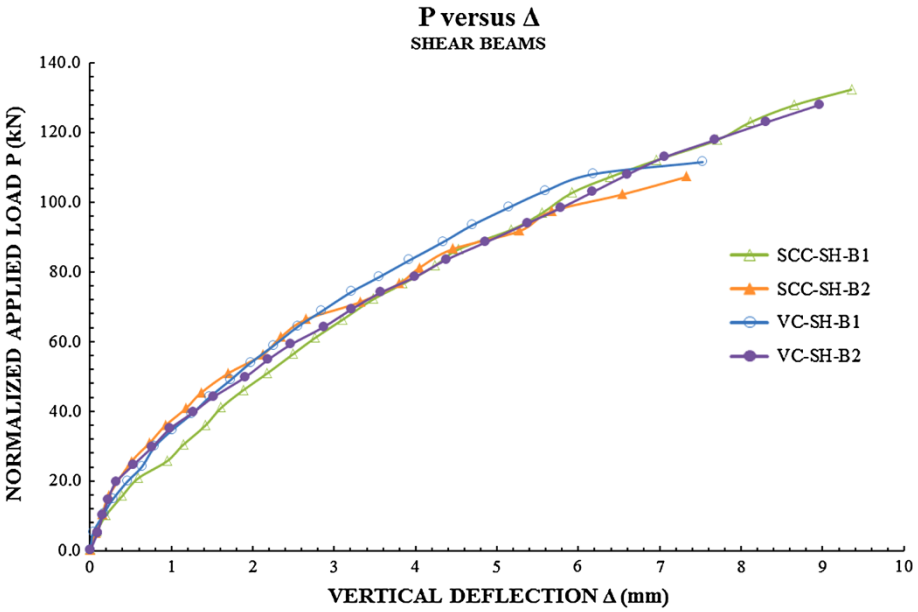

Fig. 26 Load–deflection curves of the shear beams.

indicates that the bond between steel and concrete is not affected by the high flowability of SCC mixes.

– Although several studies confirm that the shear capacity of SCC is lower than that of VC, the results of this study have demonstrated that the high consistency of SCC has no adverse effect on the shear strength of concrete. A comparison between the experimental and theoretical concrete capacities has shown an insignificant difference between the predicted and the actual shear resistances of SCC.
– The SCC and VC flexure beams exhibited similar behavior under identical loading conditions, leading to the conclusion that the high fluidity of concrete has little impact on the flexural strength of reinforced concrete beams.

Table 9 Test results of flexure beams.

Specimen notation	SCC-F-B1	SCC-F-B2	VC-F-B1	VC-F-B2
P at first diagonal crack (kN)	50	50	45	40
P at yielding (kN)	92	107	84	99
Δ_y (mm)	5.41	6.22	4.54	4.94
P at failure (kN)	158	150	155	157
Theoretical ultimate load (kN)	120	120	118	118
Δ_u (mm)	15.5	19.4	13.5	19.8
1/μ (%)	34.9	32.1	33.6	24.9
Number of cracks	14	15	15	14
Max. flexural crack width (mm)	0.6	0.6	0.6	0.6
Max. flexural crack height (cm)	23.3	23.1	22.4	20.6
Theoretical flexural crack height (cm)	21.8	21.7	21.6	21.6
Max. shear crack width (mm)	1.25	1.25	1.25	1.25

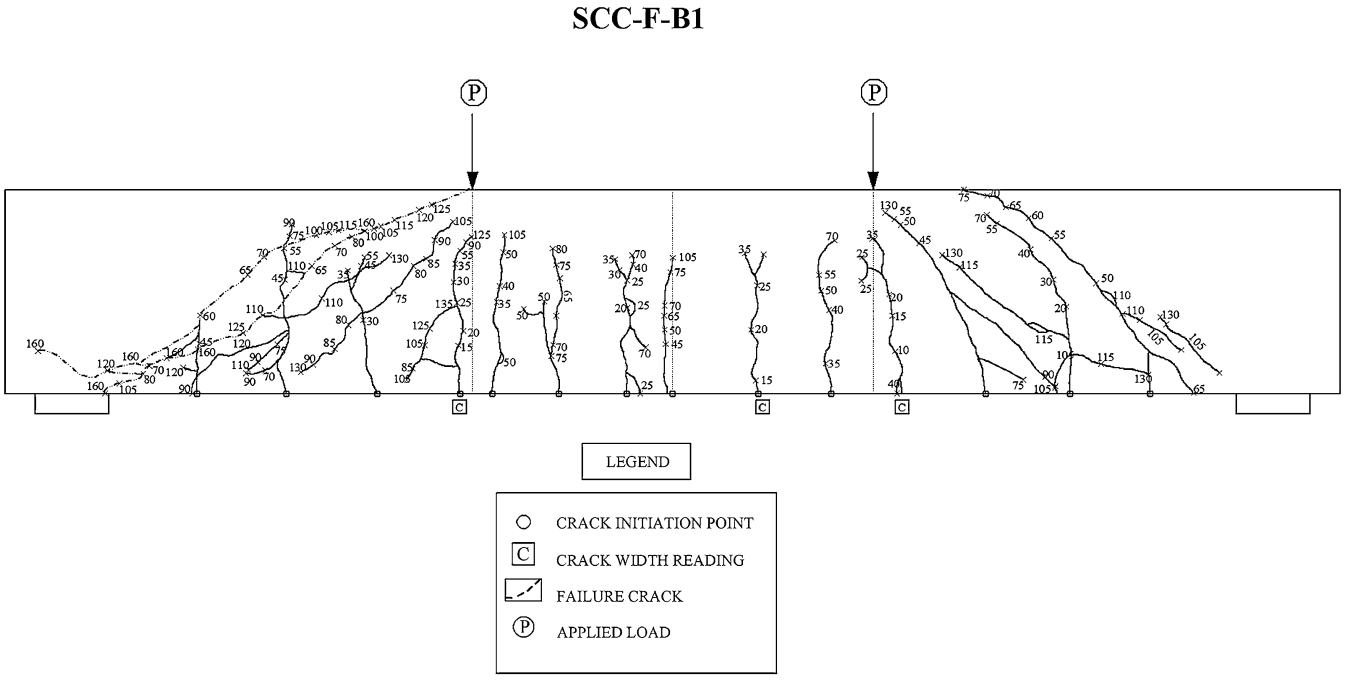

Fig. 27 Crack pattern and mode of failure associated with beam SCC-F-B1.

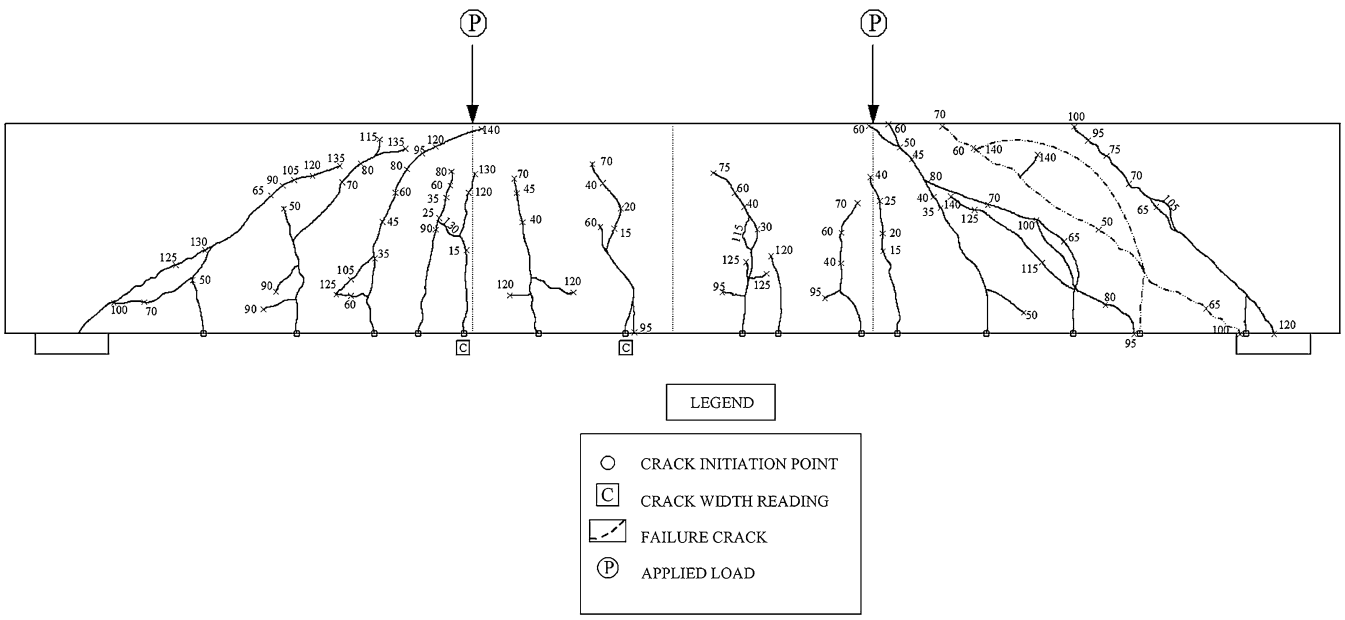

Fig. 28 Crack pattern and mode of failure associated with beam SCC-F-B2.

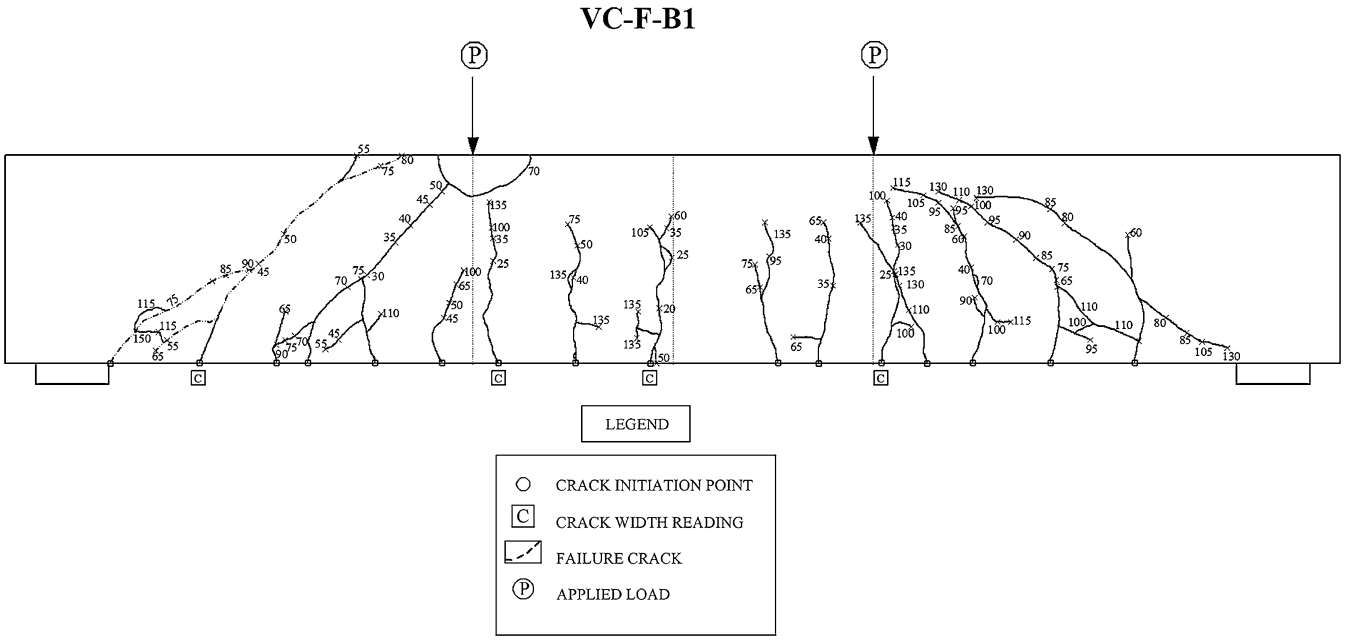

Fig. 29 Crack pattern and mode of failure associated with beam VC-F-B1.

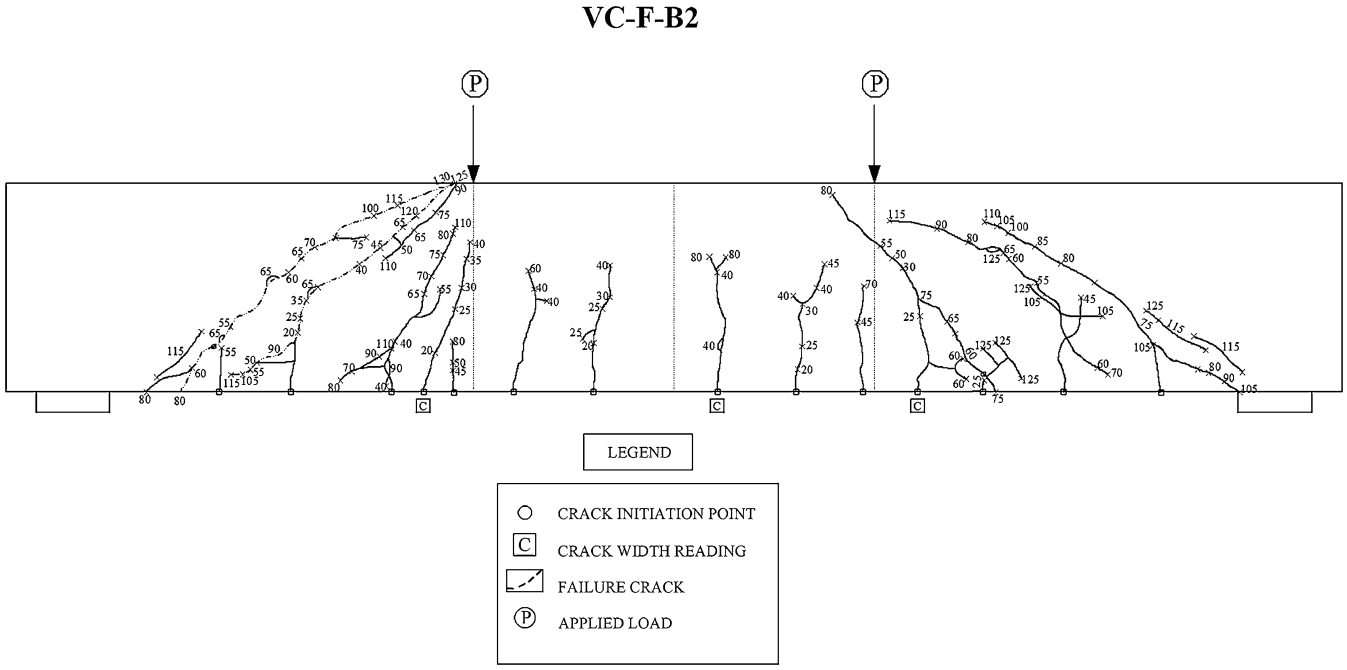

Fig. 30 Crack pattern and mode of failure associated with beam VC-F-B2.

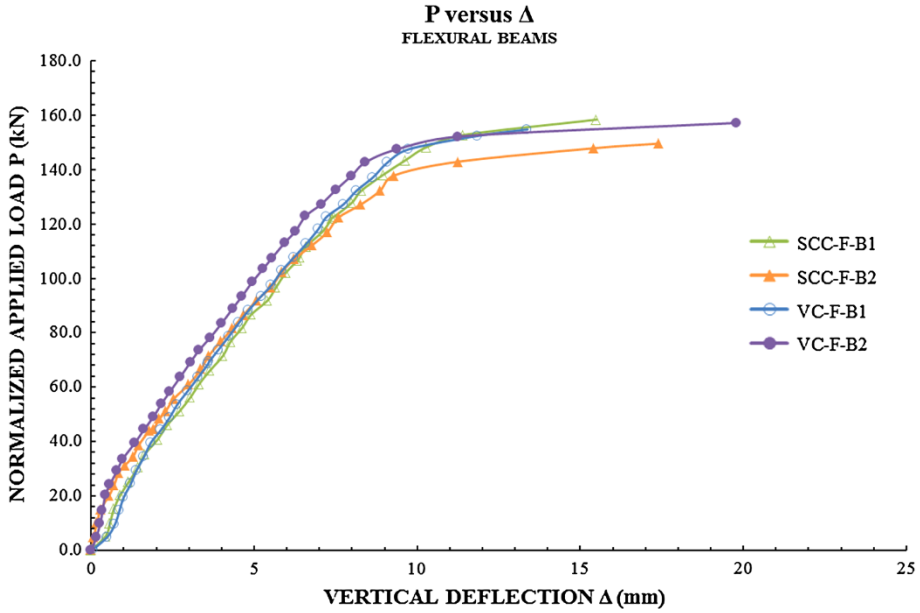

Fig. 31 Load–deflection curves of the flexural beams.

Acknowledgments

The authors gratefully acknowledge the University Research Board at the American University of Beirut for supporting this program. Also, the assistance of Mr. Helmi El-Khatib, Supervisor of the testing laboratories at AUB, is appreciated.

Open Access

References

ACI Committee 318. (2011). Building code requirements for structural concrete (ACI 318-11) and commentary. Farmington Hills, MI: American Concrete Institute.

ACI Committee 363R. (2010). Report on high strength concrete. Farmington Hills, MI: American Concrete Institute.

ACI Committee 408R. (2003). Bond and development of straight reinforcing bars in tension. Farmington Hills, MI: American Concrete Institute.

ASTM A615/A615M. (2012). Standard specification for deformed and plain carbon-steel bars for concrete reinforcement. West Conshohocken, PA: ASTM International. doi:10.1520/A0615_A0615M-12

Boel, V., Helincks, P., Desnerck, P., & De Schutter, G. (2010). Bond behaviour and shear capacity of self-compacting concrete. In *Design, production and placement of self-consolidating concrete*. Begneux, France: RILEM.

Desnerck, P., De Schutter, G., & Taerwe, L. (2010). Bond behaviour of reinforcing bars in self-compacting concrete: Experimental determination by using beam tests. *Materials and Structures, 43*, 53–62.

Domone, P. (2006). *A review of the hardened mechanical properties of self-compacting concrete*. London, UK: Cement & Concrete Association.

Domone, P. (2009). Proportioning of self-compacting concrete: The UCL method. London, UK: Department of Civil, Environmental And Geometric Engineering, University College London.

Dransfield, J. (2003). Admixtures for concrete, mortar and grout. In *Advanced concrete technology: Constituent materials*. Oxford, UK: Elsevier Butterworth Heinemann.

Foroughi-Asl, A., Dilmaghani, S., & Famili, H. (2008). Bond strength of reinforcement steel in self-compacting concrete. *International Journal of Civil Engineering, 6*(1), 24–33.

Hassan, A. A. A., Hossein, K. M. A., & Lachemi, M. (2008). Behavior of full-scale self-consolidating concrete beams in shear. *Cement & Concrete Composites, 30*(7), 588–596.

Sharifi, Y. (2012). Structural performance of self-consolidating concrete used in reinforced concrete beams. *KSCE Journal of Civil Engineering, 16*(5), 618–626.

Turk, K., Benli, A., & Calayir, Y. (2008). Bond strength of tension lap-splices in full scale self-compacting concrete beams. *Turkish Journal of Engineering and Environment Science, 32*, 377–386.